EPiC Series in Computing

Volume 62, 2019, Pages 29–47

SUMO User Conference 2019

Reinforcement Learning Agent under Partial Observability for Traffic Light Control in Presence of Gridlocks

Thanapapas Horsuwan[1] and Chaodit Aswakul[2]

[1] International School of Engineering, Faculty of Engineering, Chulalongkorn University
thanapapas@hotmail.com
[2] Wireless Network and Future Internet Research Unit,
Department of Electrical Engineering, Faculty of Engineering, Chulalongkorn University
chaodit.a@chula.ac.th

Abstract

Bangkok is notorious for its chronic traffic congestion due to the rapid urbanization and the haphazard city plan. The Sathorn Road network area stands to be one of the most critical areas where gridlocks are a normal occurrence during rush hours. This stems from the high volume of demand imposed by the dense geographical placement of 3 big educational institutions and the insufficient link capacity with strict routes. Current solutions place heavy reliance on human traffic control expertises to prevent and disentangle gridlocks by consecutively releasing each queue length spillback through inter-junction coordination. A calibrated dataset of the Sathorn Road network area in a microscopic road traffic simulation package SUMO (Simulation of Urban MObility) is provided in the work of Chula-Sathorn SUMO Simulator (Chula-SSS). In this paper, we aim to utilize the Chula-SSS dataset with extended vehicle flows and gridlocks in order to further optimize the present traffic signal control policies with reinforcement learning approaches by an artificial agent. Reinforcement learning has been successful in a variety of domains over the past few years. While a number of researches exist on using reinforcement learning with adaptive traffic light control, existing studies often lack pragmatic considerations concerning application to the physical world especially for the traffic system infrastructure in developing countries, which suffer from constraints imposed from economic factors. The resultant limitation of the agent's partial observability of the whole network state at any specific time is imperative and cannot be overlooked. With such partial observability constraints, this paper has reported an investigation on applying the Ape-X Deep Q-Network agent at the critical junction in the morning rush hours from 6 AM to 9 AM with practically occasional presence of gridlocks. The obtainable results have shown a potential value of the agent's ability to learn despite physical limitations in the traffic light control at the considered intersection within the Sathorn gridlock area. This suggests a possibility of further investigations on agent applicability in trying to mitigate complex interconnected gridlocks in the future.

1 Introduction

As the global second highest congestion level city [23], Bangkok has received numerous efforts in an attempt to alleviate the problem. In 2015, under the global initiative of the umbrella

M. Weber, L. Bieker-Walz, R. Hilbrich and M. Behrisch (eds.), SUMO2019 (EPiC Series in Computing, vol. 62), pp. 29–47

project Sustainable Mobility Project 2.0 of the World Business Council for Sustainable Development (WBCSD), the Sathorn Model Project was adopted by the Toyota Mobility Foundation in Bangkok [21]. Various sensors have been installed along the upstream lanes approaching the critical *Surasak* Intersection by the project [21]. In early attempts to mimic real world congestions for what-if scenario studies, the work of Chula-Sathorn SUMO Simulator (Chula-SSS) [3] has been initiated to provide calibrated datasets over the Sathorn Road network in a microscopic road traffic simulation package Simulation of Urban MObility (SUMO) [15]. The datasets has been extensively calibrated by the root mean squared error (RMSE) of the actual link travel time in the weekday morning and evening rush hour from 6 AM to 9 AM and 3 PM to 7 PM respectively.

One of the what-if scenarios of utmost importance is to investigate on different congestion mitigation plans especially on traffic signal light controls. In doing so, there exist numerous challenges. The Sathorn Road infrastructure stands to be the busiest road network [24]. This is due to the density of the high rise buildings and the dense geographical placement of the schools and universities. No automation has been trusted for rush-hour traffic signal light control operations, although such automation infrastructure has already been installed. Currently, in practice, a manual adaptive traffic signal control is utilized, which relies on tacit knowledge accumulated by traffic police expertise. The current traffic indicators gained through the expert's experience are the queue length and vehicle minimum gap. Although heuristic signal actuated logics were extracted from human experts as an attempt to standardize the process [3], human expertise is still heavily relied on and current tools are utilized for visualization, simulation, and further analysis. In overall, hence, the traffic signal light control problem remains an open challenge to explore further towards an optimization and automation within the present traffic signal control policies. In addition, due to severely over-saturated condition, gridlocks are a normal occurence in the time of rush hour. This requires the traffic police's manual intervention and coordination to resolve in current practices, and complicates further if such operation must be automated in the future.

In this paper, we aim to utilize the readily calibrated Chula-SSS dataset with extended vehicle flows and simulated gridlocks in order to optimize the present traffic signal control policies. The herein adopted approach is based on the reinforcement learning by an artificial agent. Reinforcement learning is a machine learning paradigm to automate goal-directed learning and decision making through an artificial agent's repeated interactions with the environment so as to maximize the cumulative numerical reward signal. And with deep reinforcement learning [16], usage of neural networks as a function approximator can be further introduced for the action-value function. With such increased generalization, it is viable for the agent to learn in large state and/or action spaces. From the literature, reinforcement learning in a traffic light control setting is not new. A number of researches utilize the Q-learning framework to apply to the traffic light control problem. The researches explored several state space definition, action space definition, and reward definitions. Various state space definition has been proposed. For instance, the state space as a dense sensory input as been seen in [9, 8], where the discrete traffic state encoding (DTSE) provides dense spatial information as 3 vectors (presense of vehicle, speed of vehicle, and traffic signal phase) to pass into a convolutional neural network. Although the dense input has shown improvements in the result, it poses a challenge towards the real-world implementation due to the dense sensor placement requirement in the real world setting. Past RL formulation of the traffic light control setting is still lacking in pragmatism, since the defined environment is a simple isolated intersection with low action space [9, 19, 8]. Although [28] attempts to utilize real-world traffic dataset from Jinan, China as the traffic flow, the environment is still an isolated intersection with 2 discrete action space. The reward

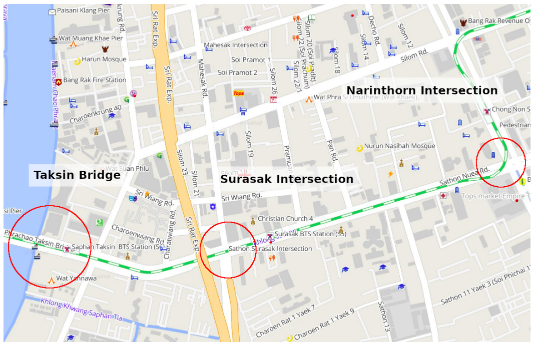

(a) Longdo Map (with granted usage permission from http://map.longdo.com/

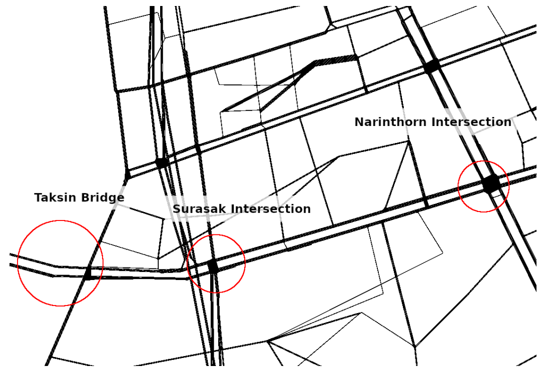

(b) Chula-SSS Dataset in SUMO

Figure 1: Comparison between actual map and Chula-SSS dataset in the Sathorn Road Area

definitions are mostly hard to observe by a real agent, such as delay [2, 6, 28, 19] or vehicle waiting time [8, 28]. There remain many open challenges consequently.

Especially for the traffic system infrastructure in developing countries, this paper tries to investigate one challenge, stemming from constraints imposed from economic factors. Particularly, this paper addresses the resultant limitation of the agent's partial observability of the whole network state at any specific time, which is imperative and cannot be overlooked. With such partial observability constraints, this paper has reported an investigation on applying the Ape-X Deep Q-Network agent at the critical junction in the morning rush hours from 6 AM to 9 AM with practically occasional presence of gridlocks. The obtainable numerical experiments utilize heavily Chula-SSS dataset with the focus on studying a potential value of the agent's ability to learn despite physical limitations in the traffic light control at the considered intersection within the Sathorn gridlock area.

The paper is organized as follows: Section 2 describes the problem and defines the agent; the experimental setup is in Section 3 and discussion of the results in Section 4; finally, we conclude the paper in Section 5.

2 Problem Formulation

In this section, we first introduce the existing traffic infrastructure, the corresponding simulation model, and then formulate the traffic light control problem as an reinforcement learning task.

2.1 Sathorn Road Infrastructure

The area of interest in the Sathorn Road network streches from the Taksin Bridge to the Witthayu intersection, which passes through the Surasak Intersection and the Narinthorn Intersection. The Chula-SSS dataset features a heavily callibrated version of the Sathorn Road network generated from OpenStreetMap (OSM). A side-by-side comparison of the actual map and the Chula-SSS dataset is shown in Figure 1. The map in the Chula-SSS Dataset has minor differences to the actual Longdo Map regarding the absence of the minor roads and the introduction of connecting sources and sinks. This was done to simplify the scope of the network

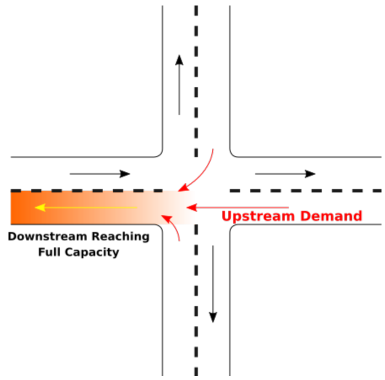

Figure 2: Example scenario for Gridlock

and to ease the manual callibration process. The vehicle flows of the dataset are callibrated only on predefined routes occuring on the major roads.

Traffic Gridlock: A traffic gridlock is a form of congestion state where queue length spillback propagates in a closed loop–resulting in a complete standstill. Once the downstream edge approaches full capacity, the limited capacity would disallow the upstream edges to enter upon a green light phase. In practice, this would lead to vehicles being trapped in the middle of the junction, blockading the path for the opposite direction–rendering any phase changes ineffective. These gridlocks are frequently observed in the Sathorn Road network at the time of peak traffic demand, requiring traffic experts to manually disentangle the gridlock through inter-junction coordination.

The Chula-SSS SUMO dataset was calibrated under SUMO v0.25.0 when the vehicle lane changing model was not properly configured, leading to criss-cross lane-to-lane connections. The vehicle behavior inside these intersecting internal links is not supported in the current SUMO v1.0.1 version. The dataset is adviced to run with the flag `--no-internal-links true`, disallowing vehicle junction blockers altogether. Although the Chula-SSS SUMO dataset was not calibrated for vehicle junction blockade, gridlocks through queue length spillback still occur for upstream demand when the downstream edge is at full capacity. In the case that the downstream capacity is full, SUMO's `no-block-heuristic` mechanism will not allow the vehicles in the upstream to move into the junction. An example scenario for gridlock can be illustrated by Figure 2, where the upstream demand from the North, West, and South directions all try to utilize the East downstream lane. If the lane capacity is not enough or there is not enough flow, the lane then becomes a traffic bottleneck and queue length spillback will occur and the vehicles in the upstream demand will be unable to flow.

The critical routes responsible for the gridlock in Chula-SSS extended flows is illustrated in Figure 3, where the vehicle routes form a closed loop on itself, potentially causing a traffic gridlock. These routes are extracted from the behavior of the parents dropping off children to their designated school and universities. Three major education institutions indicated by stars are densely located in the network. The situation is worsen by the fact that Pramuan Road and Si Wiang Road is a one-way road, imposing severe limitations on the link throughput. The Taksin Bridge serves as the connector between the West Thon Buri district and the East Sathorn district divided by the Chao Phraya River. Route 1 highlighted in red represents parents living in the East side, driving down the Sirat Expressway, dropping students and

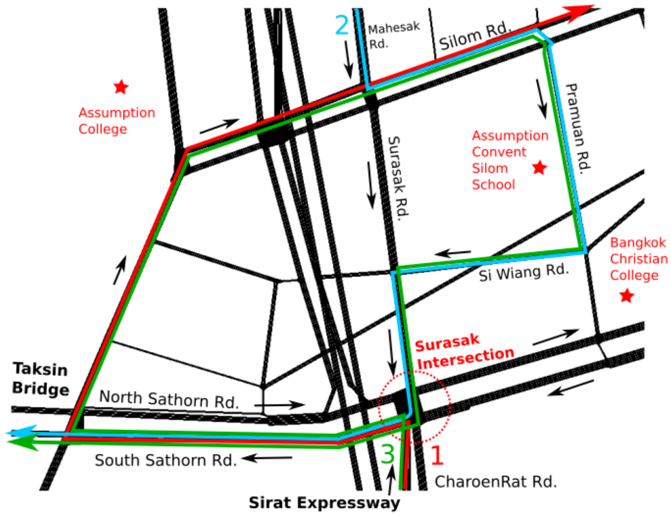

Figure 3: Critical Routes in the Sathorn Network

Table 1: Extended Route Flows

Route	Time	Flow (Vehicles per hour)	Total Vehicles
1	7:00 AM - 8:15 AM	425	531
2	6:45 AM - 7:15 AM	300	150
3	6:15 AM - 6:45 AM	300	150

proceeding to the Silom Road. Routes 2 and 3, color-coded by blue and green respectively, represents parents living in the West side–seen by the need to cross the Chao Phraya River by the Taksin Bridge. The difference between the two routes is the origin, Route 2 comes from the North Mahesak Road while Route 3 comes from the South Sirat Expressway. The flows in each route are estimated by statistical surveys at each educational institution regarding the total number of students that come by private cars as shown in Table 1. It can be observed that the 3 critical routes all utilize the downstream South Sathorn Road. It can be expected that the downstream South Sathorn Road will most likely be the bottleneck link that could potentially cause gridlock once it approaches full capacity.

The Surasak Intersection is the main junction of interest. The current traffic fixed-time control signal phase handcrafted by human experts is defined in Figure 4. The main phases as defined by the traffic police experts are phase 1, 3, and 5. However, based on the extracted heuristic signal actuated logics from human experts [3] as shown in Figure 4, extra phases which are the subset of other phases like phase 4 and 6 are also utilized in special cases to mitigate gridlock.

Sensor placement: There are a total of 3 types of sensors installed in the approaching lanes of the Surasak Intersection: induction loop coil sensors, thermal cameras, and CCTV cameras. The latter two requires image processing to extract useful information. For example, currently the camera sensors uses background subtraction to extract the vehicle occupancy data over a specific field of view of the sensor. The detailed configuration of the physical sensor placement

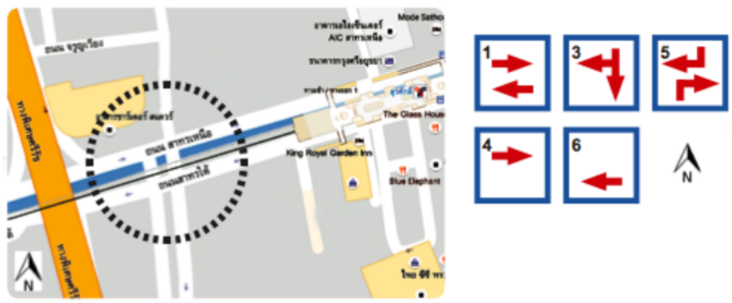

Standard Phase 1-3-1-5

Changing Phase from 1 to 3:

- When the queue of downstream North Sathorn reaches the Sathorn Intersection
- When the queue of downstream South Sathorn reaches the Sathorn Intersection
- Queue of Si Wiang Road reaches Pramuan Road on Bangkok Christian College and Assumption Convent School
- Vehicles on Taksin Bridge 300 meters from Sathorn Intersection is starting to move
- Phase 1 duration more than 120-150 seconds

Changing Phase from 3 to 1:

- Reduced jam length of Si Wiang Road or vehicles are moving on Pramuan Road continuously for 20-30 seconds
- Minimum gap between vehicles that crosses the intersection is too high
- Velocity of the vehicles that crosses the intersection is too low
- Phase 3 duration more than 30-80 seconds

Changing Phase from 1 to 5:

- Queue of Si Wiang Road reaches Pramuan Road on Bangkok Christian College and Assumption Convent School
- Queue of CharoenRat is too long
- Phase 1 duration more than 120-150 seconds

Changing Phase from 5 to 1:

- Reduced jam length of CharoenRat Road
- Phase 5 duration more than 40-50 seconds

Note: Use Phase 1-3-1-3-5 if want to get cars out from Surasak and Pramuan Road. Use Phase 4 (instead of Phase 1) when the head of queue from Sathorn South reaches Sathorn Intersection. Use Phase 6 (instead of Phase 1) when the head of queue from Sathorn North reaches Sathorn Intersection.

Figure 4: Heuristic Signal Actuated Logics at the Morning Rush Hour of Surasak Intersection [3] Version 23/11/2016 Yannawa Police District

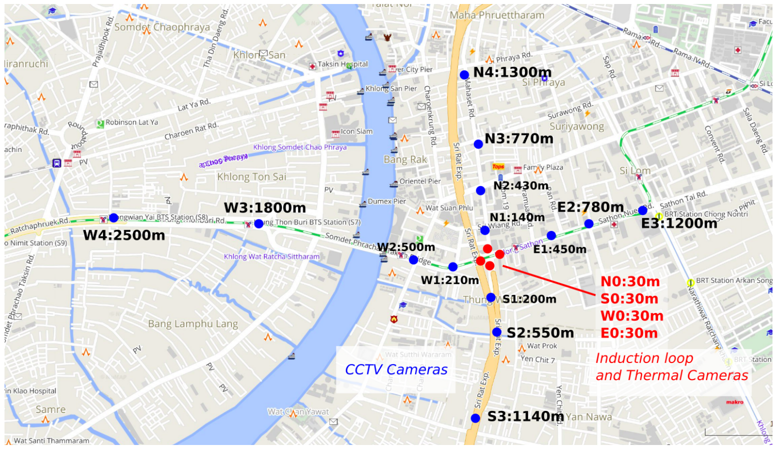

Figure 5: Sensor Configuration with granted usage permission from http://map.longdo.com/

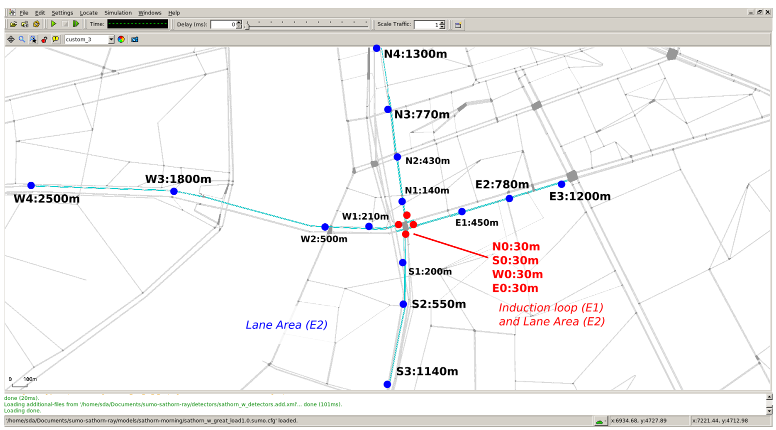

Figure 6: Detector Configuration in SUMO

is shown in Figure 5 along with the representation reflected in SUMO as shown in Figure 6. The induction loop sensors are represented by SUMO E1 Induction Loops Detectors, which are placed in the front of all the approaching upstream edges at the Surasak Intersection. The cameras of both types are represented by SUMO E2 Lane Area Detectors, from which the vehicle occupancy data over a specific area is extracted. To approximate an occupancy value over an area in SUMO, we define cell an area occupied by a set of lane area detectors representing a particular camera sensor. Each consecutive cell is continuous as opposed to the camera's specific field of view. This provides the agent with accurate information over the current cell's occupancy. Although sampling by the cameras may approximate the actual cell occupancy value, further research has to be done to verify the results. Currently there are a total of 18 cells (5 for Surasak, 4 for CharoenRat, 4 for South Sathorn, and 5 for North Sathorn). In addition, a 50-meter detector was placed in the downstream direction of each lane in the junction to expand the agent's ability to detect the aforementioned traffic gridlock via observation of queue length spilback from the downstream edges. Although these downstream edge detectors have not been made available in the actual installation on the Sathorn Road, their presence is necessary for the learning ability. And we rely on the simulation capability of SUMO together with our chosen learning algorithm to help convey this justification for future engineering investment, if a learning-based traffic light control framework would be envisioned for a possible future deployment.

2.2 Reinforcement Learning

To formulate a traffic light control as a reinforcement learning problem, we consider tasks in which an agent interacts with the envionment $\mathcal{E}$, in this case the SUMO simulation, in a sequence of observations, actions, and rewards. At each time step t the agent receives a representation of the environment's state s_t, the agent responds by selecting an action a_t, and the environment executes the action and returns back the next reward r_{t+1} and state s_{t+1}. The goal of the agent is a policy π which maximizes the expected cumulative discounted reward $R_t = \sum_{k=0}^{\inf} \gamma^k r_{t+k+1}$.

State Space

Let $\mathcal{S}_t^e$ be the environment internal state at time step t and $\mathcal{S}_t^a$ be the agent's internal representation of the state at time step t. The environment's internal state $\mathcal{S}_t^e$ is not directly observed by the agent; instead the agent observes sensory information output from the simulated detectors. The simulated detectors are placed in correspondance with the actual geographical placement of the sensors as explained in Section 2.1. Therefore, the only available observation $\mathcal{O}$ for the agent will be the occupancy values from each sensor and the current traffic signal phase P. The traffic signal phase P is a one-hot encoding of the traffic phase index, each element represents a different traffic phase, hence P is a binary vector with the size of action space $\mathcal{A}$, $P \in \mathbb{B}^{|\mathcal{A}|}$. There are a total of 21 cells in the system (18 upstream cells and 3 downstream cells). The agent's state space will then be the vector $\mathcal{S}^a \in \mathbb{R}^{21} \times P$. In SUMO, the mean occupancy for each lane area detector is defined as the mean percentage of the occupied detector's place by vehicles. However, a cell may span several edges, consisting of lane area detectors of unequal length. To find the mean occupancy, the weighted average of the mean occupancy with respect to the detector length is used.

Note that the agent has partial observability $\mathcal{O}_t = \mathcal{S}_t^a \neq \mathcal{S}_t^e$, and the agent's limited visibility does not contain enough information for the states of the other critical intersections in the grid. Although this is a partially observable Markov decision process (POMDP), we will investigate the effectiveness of the observation under the assumption that the current observation is the environment state to limit the complexity of the architecture. While it is also possible to build $\mathcal{S}_t^a$ through the complete history $\mathcal{S}_t^a = H_t$, the beliefs of the environment state $\mathcal{S}_t^a = (\mathbb{P}[\mathcal{S}_t^e = s^1], ..., \mathbb{P}[\mathcal{S}_t^e = s^n])$ [13], or using a recurrent neural network $\mathcal{S}_t^a = \sigma(\mathcal{S}_{t-1}^a W_s + \mathcal{O}_t W_0)$ [29], we will leave that up for future works to extend.

Action Space

After the agent receives a representation of the environment's state $s_t^a \in \mathcal{S}$ at the beginning of time step t, the agent is required to select an action $a_t \in \mathcal{A}$ to influence the system dynamics. The action space $\mathcal{A}$ is the set of all possible actions that the agent is allowed to take. As shown in Figure 7, the action space $\mathcal{A} = \{0, ..., 8\}$ is the set of all traffic signal phases. This action space is extended from the list of selected actions from human experts, accounting for all the subsets and possible combinations of the phases. The environment dynamics will change according to the selected action. If the chosen action a_t is the same with the previous action a_{t-1}, then the traffic lights at that time remain unchanged. If the chosen action a_t is different from the

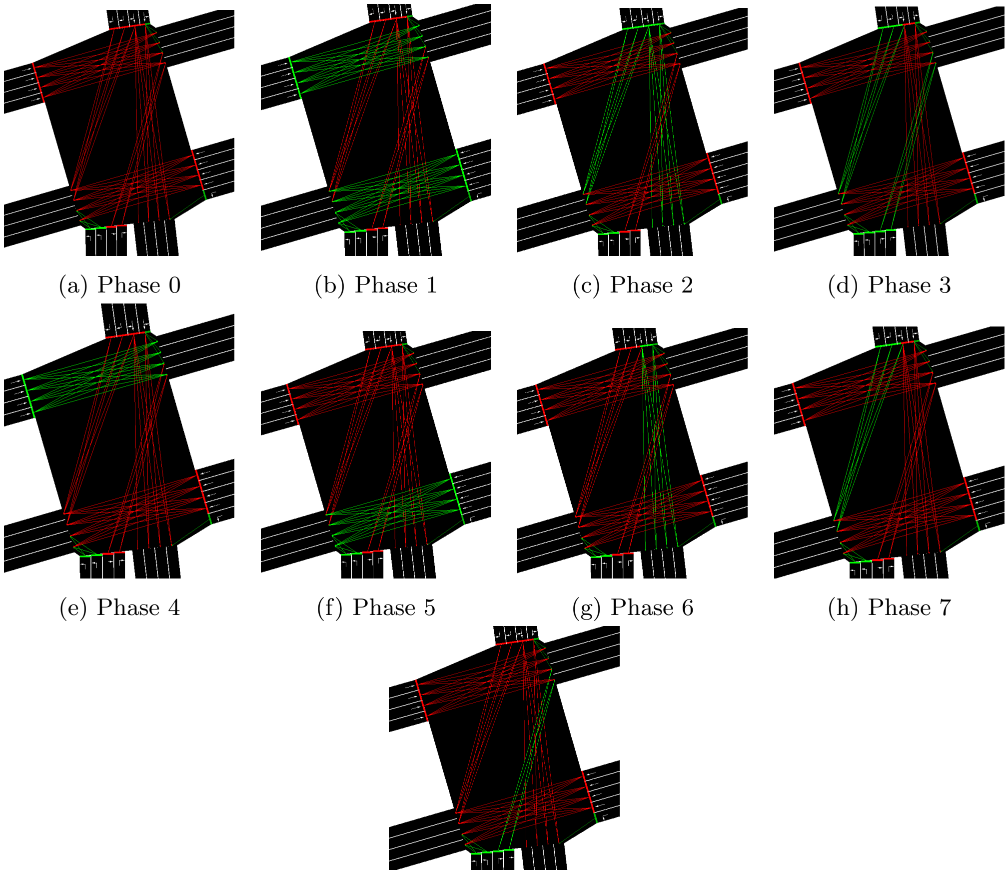

(a) Phase 0 (b) Phase 1 (c) Phase 2 (d) Phase 3
(e) Phase 4 (f) Phase 5 (g) Phase 6 (h) Phase 7
(i) Phase 8

Figure 7: Action Space Consisting of 9 Phases

previous action a_{t-1}, then a transition of traffic signal is executed before the selected action a_t. The transition signal is defined as 5 seconds of yellow light for lanes that have previously received green light.

Reward

The immediate feedback signal after the agent takes an action a_t is the scalar reward $r_{t+1} \in \mathbb{R}$. With the limited visibility of the agent, the reward r_{t+1} in this research is shown in Equation (1): the weighted difference between the vehicle throughput during time step t to $t+1$ denoted by μ_{t+1} and weighted observed occupancy. The vehicle throughput is provided by the induction loop detectors, and the weighted observed occupancy is from the observation in the next time step $\mathcal{O}_{t+1}$. Note that the use of the subscript $t+1$ in the reward is intentional as to place emphasis on the chronological flow of receiving delayed reward the time step after taking an action a_t, by which the agent is able to observe the new state s_{t+1}.

$$r_{t+1} = \alpha \mu_{t+1} - \beta(\mathcal{O}_{t+1} \cdot C) \tag{1}$$

whereby $\alpha \in \mathbb{R}^+$ and $\beta \in \mathbb{R}^+$ are non-negative constants to vary the ratio between the two terms. As defined in the agent's state, the observation vector $\mathcal{O} \in \mathbb{R}^{21} \times P$ comprises of 18 occupancy values for each upstream cell, 3 occupancy values for each downstream cell, and the one-hot encoding of the traffic signal phase. To limit the agent's punishment for vehicles that are too far away, only the first 3 cells in each upstream approaching cells are taken into account. The occupancy values from the observation vector will then be dot product by the maximum cell capacity C, which is a vector containing the maximum cell capacity for the first 3 upstream approaching cells. The maximum cell capacity is defined as the maximum number of vehicles that is able to fit inside a cell without minimum gap length. The resulting product would give the total vehicle backlog of all of the approaching lanes with respect to the 3 approaching cells.

In this paper, we will investigate the effects of varying the parameters α and β in the reward function.

Agent Architecture

We model the learning agent to learn in a distributed setting with Ape-X [11]. The Ape-X architecture is a general learning framework which centralizes a shared replay memory and uses prioritized experience replay [20] to learn the most useful experiences. Different exploration policies can be given to the different distributed actors. This framework may be combined with different learning algorithms, where we have combined it with Deep Q network (DQN) [16, 17] without the convolutional layers due to the low spatial dimensionality of the input. With the numerous improvements and proposed extensions to the architecture [25, 26, 20, 4, 7], we have chosen to utilize some of the extensions of Rainbow [10] as proposed in Ape-X DQN.

Vanilla DQN: A deep Q network (DQN) is a multi-layered neural network that estimates the action-value function $Q(s, a; \theta) \approx Q^*(s, a)$, with θ as the parameters. Two important components of the DQN are the experience replay and the target slowly moving copy of the online network with parameters θ^- [17]. The experience replay [12] stores the agent's experiences $e_t = (s_t, a_t, r_t, s_{t+1})$ and batches are sampled from the pool uniformly ie. $(s, a, r, s') \sim U(D)$. The notation without t is to denote that the sampled experience need not be at the current time t, but any experience from the replay buffer. The Q network can be trained by adjusting the parameters θ_t to reduce the mean-squared error in the Bellman equation. The following loss function at training step t is the squared Temporal Difference (TD) error.

$$L_t(\theta_t) = \frac{1}{2}\mathbb{E}_{(s,a,r,s')\sim U(D)}\left[\left(r + \gamma \max_{a'} Q(s', a'; \theta_t^-) - Q(s, a; \theta_t\right)^2\right]$$

Ape-X DQN: The extensions that we have chosen from Rainbow [10] includes: Double Q-Learning [25] to lower the overestimation bias due to the use of the max operator, Prioritized Replay [20] to increase data efficiency of the samples by importance weighted with absolute TD error, Dueling Networks [26] to improve the generalization of the agent by learning the value of each state, and Multi-step learning [22] for faster convergence.

Ape-X DQN [11] combines the aforementioned improvements in a single integrated agent. A dueling network architecture is used as the function approximator $Q(\cdot, \cdot, \theta)$. The loss function is then:

$$L_t(\theta_t) = \frac{1}{2}\mathbb{E}_{(s,a,r,s')\sim p_t(D)}\left[\left(r^{(n)} + \gamma^n Q(s^{(n)}, \operatorname*{argmax}_a Q(s^{(n)}, a; \theta_t), \theta_t^-) - Q(s, a; \theta_t\right)^2\right]$$

where the experience $(s, a, r, s') \sim p_t(D)$ is sampled in a prioritized experience replay manner and p_t denotes the probability distribution of selecting an experience. The superscript (n) denotes the n-step learning.

3 Experimental Setup and Training

The experiments have been conducted by using RISELab's RLlib [14], an open-source library for reinforcement learning that uses Ray [18] for distributed execution and Tensorflow [1] for model definition. We have built an OpenAI Gym [5] wrapper around the Chula-SSS dataset [3] and SUMO v1.0.1 [15] interfaced with Libsumo–a Traci API [27] C++ interface for interaction with the running simulation with language bindings for Python via SWIG.

One episode is defined as one full run of the Chula-SSS morning dataset–a 3 hour simulated traffic from 6AM to 9AM consisting of 10800 simulation steps (one simulation step corresponds to 1 simulated second by configuring `--step-length 1` when running SUMO). We train for a total of 250 training epoch, where each epoch is 43200 simulation steps (equivalent to 4 episodes, but the number of episodes completed per epoch is non-uniform due to the asynchronous training). In total, the agent will accumulate experience equal to a total of 1000 episodes (10.8 million simulated steps) or 3000 hours of experience, equivalent to 125 simulated days. An agent step or agent's action interval is defined to be equivalent to 10 simulation steps ie. an agent is allowed to take an action every 10 seconds.

Each experiment has been executed on the Google Cloud Platform (GCP) with a Compute Engine Instance of 24 vCPUs, 64 GB Memory, and 1 Nvidia Tesla P4. At any given point in time, there will be 23 actors and 1 learner running in parallel for each agent.

For the reward function parameters, α is kept constant at 1 while β is varied linearly from 0.04 to 0.16 in intervals of 0.04. This interval is chosen since in the beginning of training, the average throughput in an episode was measured to be 57 ± 20 while the average weighted occupancy in an episode was measured to be 720 ± 360. A rough coefficient to multiply the weighted occupancy with so that both variables have comparable importance is approximated to be $57/720 \approx 0.08$. The discount factor γ used is 0.9. Training uses the Adam optimizer with the learning rate of $5 * 10^{-4}$. A forward-view multi-step learning is used with a truncated 3-step return. A buffer size of 1 million is used in the experience replay. The absolute TD errors are used for the learner's replay sampling priorities, which are sampled by with priority exponent $\alpha_{sample} = 0.6$. The prioritized replay bias is corrected with the importance sampling factor of $\beta = 0.4$. The exploration fraction ϵ is annealed from 1 to 0.1 in 150k timesteps. Gradient norms are clipped to 40. Before the learning starts, the learner waits for 10800 steps to be accumulated in the experience replay. The target network used in the loss calculation is copied from the online network every 21600 steps or 10 episodes.

4 Results and Discussion

The performance of the agent is assessed for both the agent's observable and non-observable metrics: reward, throughput, jam length, mean speed, and average green time. One justification of the agent's learning performance with respect to average reward per episode is shown in Figure 8. At the end of the training, the reward signal remains stagnant, which indicates a convergent behavior for all parameter cases of the agent. The convergence behavior between all cases seem to be similar, plateauing at around 400k agent steps.

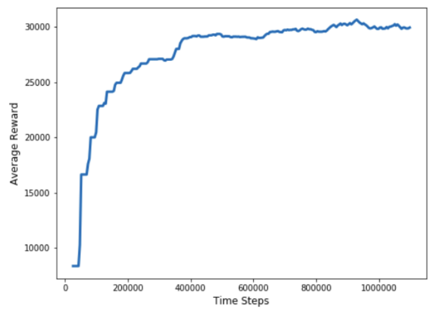

(a) Reward α=1 β=0.04

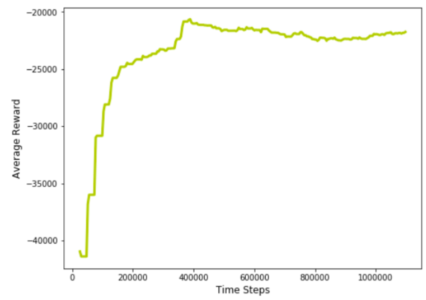

(b) Reward α=1 β=0.08

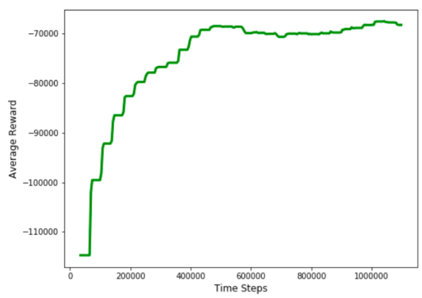

(c) Reward α=1 β=0.12

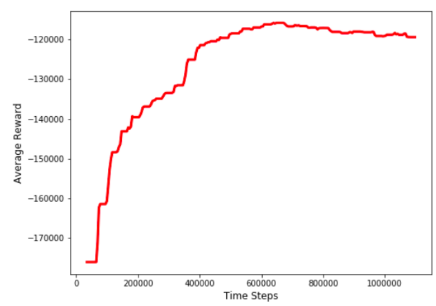

(d) Reward α=1 β=0.16

Figure 8: Reward of Different Parameters

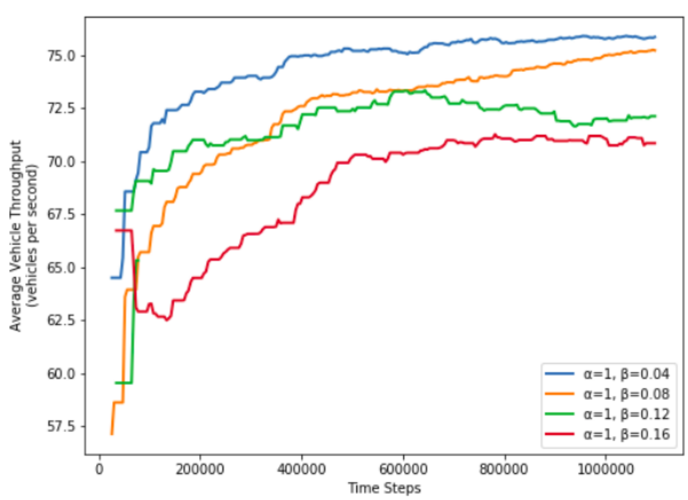

Figure 9: Average Vehicle Throughput

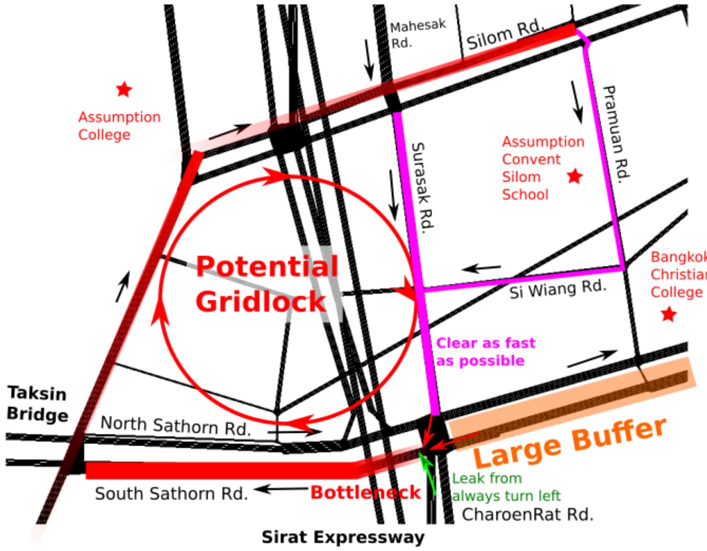

Figure 10: Potential Visual Policy of the Sathorn Road Network

The agent's average vehicle throughput is shown in Figure 9. It is expected that the order of the vehicle throughput at the end of 1 million agent steps would be in the inverse order of the weighted occupancy coefficient. This is because the more importance it places to the vehicle backlog from the β term, the less important the vehicle throughput provided by the α term is. At 800k agent steps, it is evident that the agent with $\beta = 0.04$ has the highest throughput and $\beta = 0.08, 0.12, 0.16$ in decreasing order. This shows the agent's ability to be able to place importance in the concerning factors of the reward function.

An interesting insight could be seen in Figure 11. All the parameter cases of the agent favor the lower jam length in the Surasak upstream lanes and place low importance in decreasing the South Sathorn jam length. An average Surasak jam length lower than 300 meters is observed in all cases after 600k agent steps, and South Sathorn jam length being over 500 meters after 400k agent steps. There is a slight change in this particular behavior when the importance in weighted occupancy term β is increased, allowing Surasak's jam length to increase when comparing $\beta = 0.04, 0.08$ and $\beta = 0.12, 0.16$. This policy is in agreement of the traffic police expert's technique, using South Sathorn as the buffer zone to block the vehicles that could potentially enter the critical loop, while giving high priority to the Surasak upstream direction to be able to alleviate the potential gridlock as discussed in Section 2.1. The policy could be further visualized in Figure 10. It can be seen that congestion in the the upstream of the South Sathorn Road will likely not affect the current gridlock of interest, and with the large capacity of the link, the agent is able to treat it as a buffer to allow cars to fill in without allowing them to proceed to the bottleneck downstream link of the South Sathorn Road. On the other hand, the Surasak Road directly affects the potential gridlock that could happen and a high jam length could rapidly propagate the queue-length spillback to the other links. The Surasak Road should be taken care off quickly as a result.

The North Sathorn jam length suggests a slightly decreasing trend. In accordance to the aforementioned critical gridlock loop, there is no drawback in releasing the North Sathorn Road to the downstream link as the vehicles will not contribute to the gridlock. The CharoenRat jam

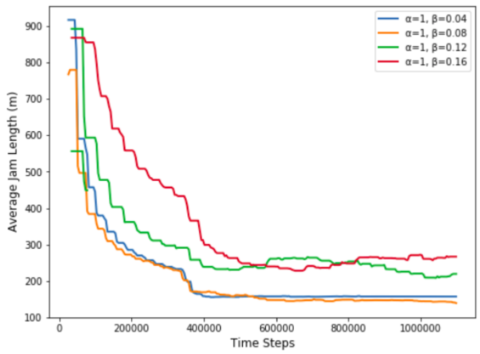

(a) Surasak Jam Length

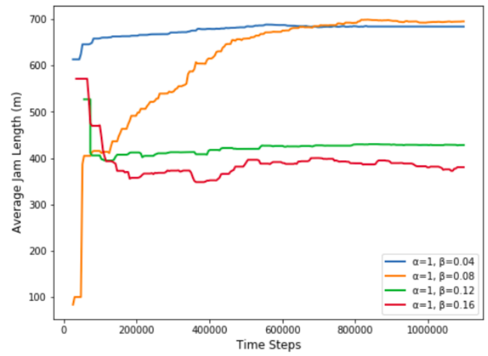

(b) CharoenRat Jam Length

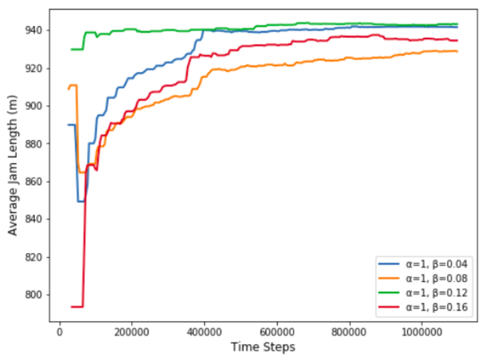

(c) South Sathorn Jam Length

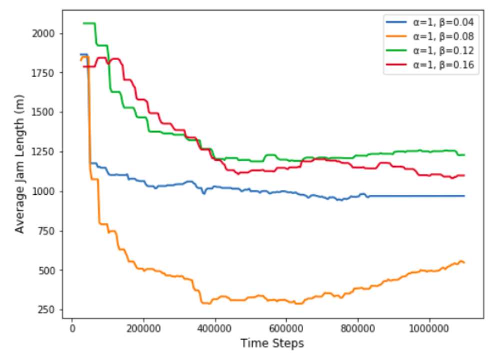

(d) North Sathorn Jam Length

Figure 11: Jam Length of the Approaching Lanes

length divides into two courses of action: the two agents with the lower weighted occupancy coefficient $\beta = 0.04, 0.08$ allows the jam length in the CharoenRat direction to be at around 700 meters, while the other two agents with the higher weighted occupancy coefficient $\beta = 0.12, 0.16$ controls the jam length to be around 400 meters. This should be seen in conjunction with the average green time in Figure 12. The agent with higher weighted occupancy $\beta = 0.12, 0.16$ does not allow the vehicles in the CharoenRat Road to fill up, as it would mean the increase of the total number of vehicles existent on the road. This is observed by the average green time of phases 3 and 8 in Figure 12d and Figure 12i respectively. The agent with the higher weighted occupancy $\beta = 0.12, 0.16$ has an average green time on phases 3 and 8 at around 20 seconds, while the agents with the lower weighted occupancy $\beta = 0.04, 0.08$ has much lower green time on these phases. Although the higher weighted occupancy agents favor the upstream of CharoenRat, the consistent average jam length of around 400 meters comes from the fact that CharoenRat is divided into two sections: the two leftmost lanes in the CharoenRat Road is always turn left and the two rightmost lanes in the CharoenRat Road is always turn right. Hence, the agent has no control over the vehicle leakage and the average jam length will always be existent if there is high queue length spillback in the downstream edge of South Sathorn and the flow of vehicles from the CharoenRat Road attempting to enter the critical loop exists.

The mean speed in Figure 13 suggests relatively similar insights with the jam length. The Surasak junction achieving high mean speed, and the South Sathorn experiences drastically low

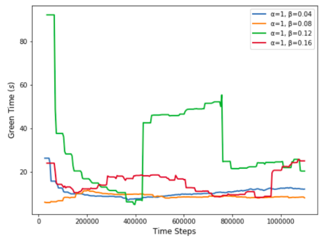

(a) Average Green Time of Phase 0

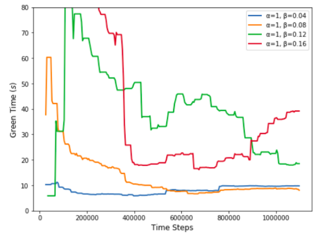

(b) Average Green Time of Phase 1

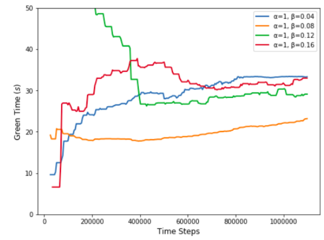

(c) Average Green Time of Phase 2

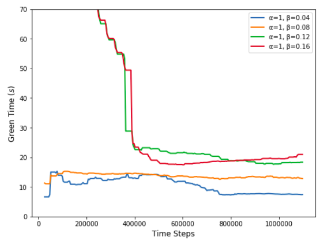

(d) Average Green Time of Phase 3

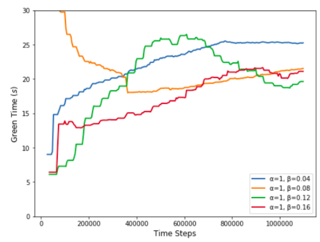

(e) Average Green Time of Phase 4

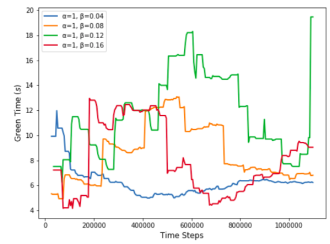

(f) Average Green Time of Phase 5

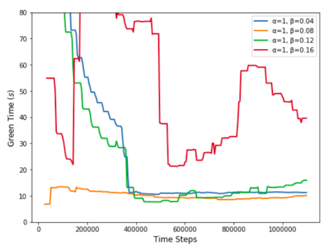

(g) Average Green Time of Phase 6

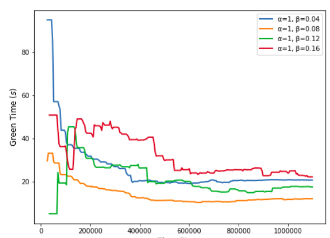

(h) Average Green Time of Phase 7

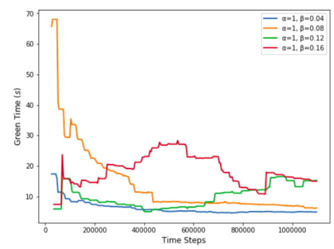

(i) Average Green Time of Phase 8

Figure 12: Average Green Time of the 9 Phases

mean speed. The reasoning should be similar to what was previously mentioned, the Surasak Road being of crucial importance and the South Sathorn as an idle buffer. North Sathorn experiences a slight increase in mean speed and CharoenRat separates into two cases due to the shifted importance of the reward weights: the higher weighted occupancy $\beta = 0.12, 0.16$ achieving a higher mean speed while the lower weighted occupancy $\beta = 0.04, 0.08$ achieves a lower mean speed.

The average green time of the different phases in Figure 12 provides more insight to the agent's actions. The phases that all the agents are in agreement are phases 2 and 4, which has a clear increasing trend of being assigned green time. Phase 2 corresponds to releasing the upstream supply of Surasak to all the downstream edges. As discussed earlier, the Surasak Road is the road that should be given most importance with respect to the potential gridlock. Approaching 1 million agent steps, all agents agree to give phase 2 an average green time of more than 25 seconds. Phase 4 has a lower average green time of around 18 seconds, which corresponds to the phase in releasing only the upstream supply of North Sathorn. The downstream of North Sathorn does not contribute to the gridlock in anyway, and it is logical

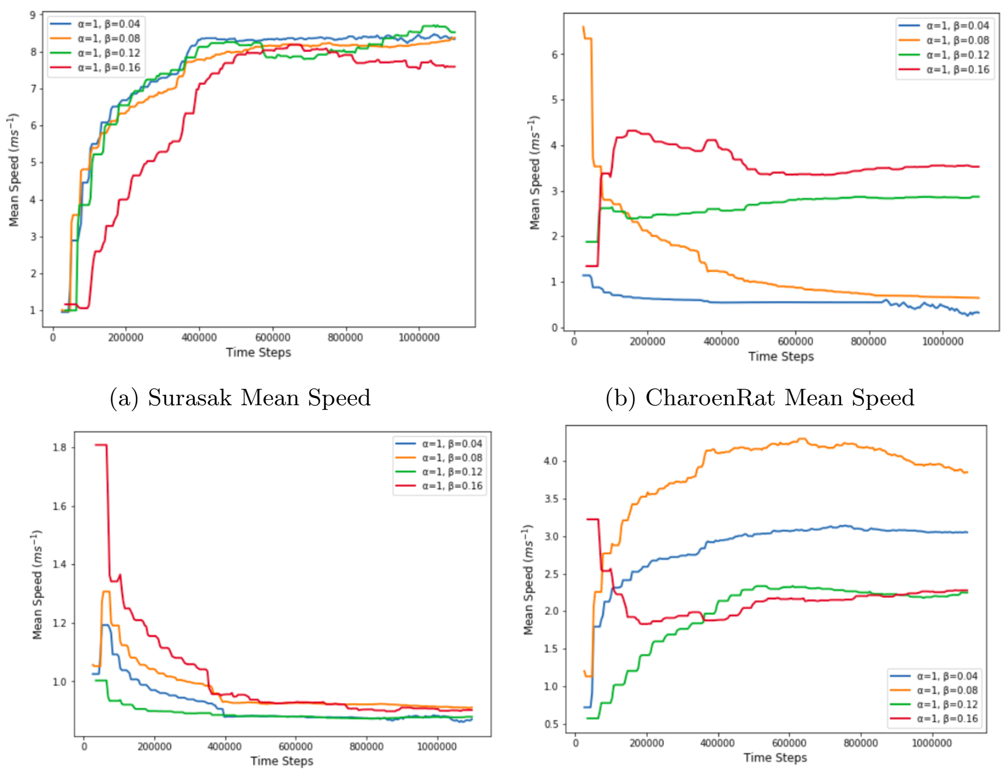

(a) Surasak Mean Speed

(b) CharoenRat Mean Speed

(c) South Sathorn Mean Speed

(d) North Sathorn Mean Speed

Figure 13: Mean Speed of the Approaching Lanes

that the agents learn that there is no harm in releasing the North Sathorn upstream. There are some phases which the agent are not in agreement with each other, for example: Phase 1, where the agents with higher weighted occupancy values $\beta = 0.12, 0.16$ favor to keep green time more than 20 seconds, while the agent with lower values $\beta = 0.04, 0.08$ consistently keep the green time at 10 seconds. Phase 1 is the phase that releases both the upstream of North Sathorn and the upstream of South Sathorn simultaneously. Although this is theoretically more efficient than Phase 4 where it releases only one upstream, it has severe drawbacks when the downstream is near full capacity and may lead to queue length spillback–contributing to gridlock. However, since the agent with higher β values are more sensitive to vehicle backlog, it would prefer to release the upstream supply of the Sathorn South direction to reduce the South Sathorn buffer in expense of a potential gridlock. Phase 5 is an interesting phase, since it is the phase that releases the upstream Sathorn South buffer to the bottleneck downstream. It seems like the agents are undecided on the results of this phase, resulting in a high variance in the graph. However, the average green time of phase 5 at around 10 seconds, which is low comparative to the other phases. Phase 0 is also interesting, where it is an all red phase. The agents with higher weighted occupancy values $\beta = 0.12, 0.16$ seem to favor the all red phase much more than the lower values. This is because it places less importance on the vehicle throughput, lowering the incentive to switch lights to make vehicles flow. This may imply that the agents are able to be idle and wait for quite a while before selecting a useful action. Phase

7 seems pretty stationary at around the average green time of 20 seconds. Phase 6 is more special, where only the highest weighted occupancy value $\beta = 0.16$ favors with more than 30 seconds of average green time. We have no explanation on why this occurs.

5 Conclusion

We have tested an artificial traffic lights controller Ape-X DQN agent under partial observability with limited sensory inputs in the traffic microsimulator SUMO. The Chula-SSS data with extended flows is used to trigger gridlock behavior as a base environment for the agent to learn. Results regarding the exploration with the reward being the weighted difference between the vehicle throughput and vehicle backlog (weighted occupancy) has been reported. The results show that the agent is able to derive insights and gridlock alleviation techniques similar to that of the traffic police experts even with no information about the whole gridlock state of all the critical looped road segments. However, the experiments reported on this paper are very limited with few hyperparameters tuning. Future works may continue to research further and do extensive ablation tests on the hyperparameters settings.

Future works can explore the agent's reaction to the different constraints and limitations to the agent's observability, and see how the agent changes its learning behaviors over each additional sensory input. This could prove to be useful in third world countries where sensors are scarce. Additionally, the reward function should also be worth further explorations for different combinations and formulation to increase the agent's effectiveness when dense reward information signals are not available. The load factor for extended flows contributing to the gridlock loop can also be varied to observe the breakdown conditions and the optimal conditions with respect to the extent of the agent's abilities for traffic light control.

This paper has demonstrated the capability of the agent to incur insightful actions for a larger problem with very limited knowledge. This capability of the agent can extend to further researches and potentially aid people to make more informed decisions for investment on sensors.

References

[1] Martín Abadi, Ashish Agarwal, Paul Barham, Eugene Brevdo, Zhifeng Chen, Craig Citro, Greg S. Corrado, Andy Davis, Jeffrey Dean, Matthieu Devin, Sanjay Ghemawat, Ian Goodfellow, Andrew Harp, Geoffrey Irving, Michael Isard, Yangqing Jia, Rafal Jozefowicz, Lukasz Kaiser, Manjunath Kudlur, Josh Levenberg, Dan Mané, Rajat Monga, Sherry Moore, Derek Murray, Chris Olah, Mike Schuster, Jonathon Shlens, Benoit Steiner, Ilya Sutskever, Kunal Talwar, Paul Tucker, Vincent Vanhoucke, Vijay Vasudevan, Fernanda Viégas, Oriol Vinyals, Pete Warden, Martin Wattenberg, Martin Wicke, Yuan Yu, and Xiaoqiang Zheng. TensorFlow: Large-scale machine learning on heterogeneous systems, 2015. Software available from tensorflow.org.

[2] Itamar Arel, Cuibi Liu, T. Urbanik, and A. G. Kohls. Reinforcement learning-based multi-agent system for network traffic signal control. *IET Intelligent Transport Systems*, 4(2):128–135, June 2010.

[3] Chaodit Aswakul, Sorawee Watarakitpaisarn, Patrachart Komolkiti, Chonti Krisanachantara, and Kittiphan Techakittiroj. Chula-sss: Developmental framework for signal actuated logics on sumo platform in over-saturated sathorn road network scenario. In Evamarie Wießner, Leonhard Lücken, Robert Hilbrich, Yun-Pang Flötteröd, Jakob Erdmann, Laura Bieker-Walz, and Michael Behrisch, editors, *SUMO 2018- Simulating Autonomous and Intermodal Transport Systems*, volume 2 of *EPiC Series in Engineering*, pages 67–81. EasyChair, 2018.

[4] Marc G. Bellemare, Will Dabney, and Rémi Munos. A Distributional Perspective on Reinforcement Learning. *arXiv e-prints*, page arXiv:1707.06887, Jul 2017.

[5] Greg Brockman, Vicki Cheung, Ludwig Pettersson, Jonas Schneider, John Schulman, Jie Tang, and Wojciech Zaremba. Openai gym, 2016.

[6] Samah El-Tantawy, Baher Abdulhai, and Hossam Abdelgawad. Multiagent reinforcement learning for integrated network of adaptive traffic signal controllers (marlin-atsc): Methodology and large-scale application on downtown toronto. *IEEE Transactions on Intelligent Transportation Systems*, 14(3):1140–1150, Sep. 2013.

[7] Meire Fortunato, Mohammad Gheshlaghi Azar, Bilal Piot, Jacob Menick, Ian Osband, Alex Graves, Vlad Mnih, Remi Munos, Demis Hassabis, Olivier Pietquin, Charles Blundell, and Shane Legg. Noisy Networks for Exploration. *arXiv e-prints*, page arXiv:1706.10295, Jun 2017.

[8] Juntao Gao, Yulong Shen, Jia Liu, Minoru Ito, and Norio Shiratori. Adaptive Traffic Signal Control: Deep Reinforcement Learning Algorithm with Experience Replay and Target Network. *arXiv e-prints*, page arXiv:1705.02755, May 2017.

[9] Wade Genders and Saiedeh Razavi. Using a Deep Reinforcement Learning Agent for Traffic Signal Control. *arXiv e-prints*, page arXiv:1611.01142, Nov 2016.

[10] Matteo Hessel, Joseph Modayil, Hado van Hasselt, Tom Schaul, Georg Ostrovski, Will Dabney, Dan Horgan, Bilal Piot, Mohammad Azar, and David Silver. Rainbow: Combining Improvements in Deep Reinforcement Learning. *arXiv e-prints*, page arXiv:1710.02298, Oct 2017.

[11] Dan Horgan, John Quan, David Budden, Gabriel Barth-Maron, Matteo Hessel, Hado van Hasselt, and David Silver. Distributed Prioritized Experience Replay. *arXiv e-prints*, page arXiv:1803.00933, Mar 2018.

[12] Long ji Lin. Self-improving reactive agents based on reinforcement learning, planning and teaching. In *Machine Learning*, pages 293–321, 1992.

[13] Leslie Pack Kaelbling, Michael L. Littman, and Anthony R. Cassandra. Planning and acting in partially observable stochastic domains. *Artif. Intell.*, 101(1-2):99–134, May 1998.

[14] Eric Liang, Richard Liaw, Robert Nishihara, Philipp Moritz, Roy Fox, Ken Goldberg, Joseph E. Gonzalez, Michael I. Jordan, and Ion Stoica. RLlib: Abstractions for distributed reinforcement learning. In *International Conference on Machine Learning (ICML)*, 2018.

[15] Pablo Alvarez Lopez, Michael Behrisch, Laura Bieker-Walz, Jakob Erdmann, Yun-Pang Flötteröd, Robert Hilbrich, Leonhard Lücken, Johannes Rummel, Peter Wagner, and Evamarie Wießner. Microscopic traffic simulation using sumo. In *The 21st IEEE International Conference on Intelligent Transportation Systems*. IEEE, 2018.

[16] Volodymyr Mnih, Koray Kavukcuoglu, David Silver, Alex Graves, Ioannis Antonoglou, Daan Wierstra, and Martin Riedmiller. Playing Atari with Deep Reinforcement Learning. *arXiv e-prints*, page arXiv:1312.5602, Dec 2013.

[17] Volodymyr Mnih, Koray Kavukcuoglu, David Silver, Andrei A. Rusu, Joel Veness, Marc G. Bellemare, Alex Graves, Martin Riedmiller, Andreas K. Fidjeland, Georg Ostrovski, Stig Petersen, Charles Beattie, Amir Sadik, Ioannis Antonoglou, Helen King, Dharshan Kumaran, Daan Wierstra, Shane Legg, and Demis Hassabis. Human-level control through deep reinforcement learning. *Nature*, 518(7540):529–533, February 2015.

[18] Philipp Moritz, Robert Nishihara, Stephanie Wang, Alexey Tumanov, Richard Liaw, Eric Liang, Melih Elibol, Zongheng Yang, William Paul, Michael I. Jordan, and Ion Stoica. Ray: A Distributed Framework for Emerging AI Applications. *arXiv e-prints*, page arXiv:1712.05889, Dec 2017.

[19] Seyed Sajad Mousavi, Michael Schukat, and Enda Howley. Traffic Light Control Using Deep Policy-Gradient and Value-Function Based Reinforcement Learning. *arXiv e-prints*, page arXiv:1704.08883, Apr 2017.

[20] Tom Schaul, John Quan, Ioannis Antonoglou, and David Silver. Prioritized Experience Replay. *arXiv e-prints*, page arXiv:1511.05952, Nov 2015.

[21] Angkee Sripakagorn, Sorawit Narupiti, Yutaka Okayama, Chayadit Kittankajon, Sunhapos Chatranuwathana, Nuksit Noomwongs, Thitipat Thitacharee, Wachhira Nilprapunt, Soravas Treenok, and Sakchai Naphapunsakul. Sathorn model summary report. Toyota Mobility Foun-

dation. https://drive.google.com/file/d/1cxOWsOAJQNZiNtjxeyp9BATVPvBN96Mj/view, 2017. Accessed: 2019-03-03.

[22] Richard S. Sutton and Andrew G. Barto. *Reinforcement learning - an introduction.* Adaptive computation and machine learning. MIT Press, 1998.

[23] The Netherlands TomTom N.V. Dutch Company, Amsterdam. Tomtom traffic index: Bangkok, thailand. https://www.tomtom.com/en_gb/trafficindex/city/bangkok, 8 2016. Accessed: 2019-03-03.

[24] Traffic and Transportation Department. Traffic statistics 2015. Technical report, Bangkok Metropolitan Administration, 2016.

[25] Hado van Hasselt, Arthur Guez, and David Silver. Deep Reinforcement Learning with Double Q-learning. *arXiv e-prints*, page arXiv:1509.06461, Sep 2015.

[26] Ziyu Wang, Tom Schaul, Matteo Hessel, Hado van Hasselt, Marc Lanctot, and Nando de Freitas. Dueling Network Architectures for Deep Reinforcement Learning. *arXiv e-prints*, page arXiv:1511.06581, Nov 2015.

[27] Axel Wegener, Michal Piorkowski, Maxim Raya, Horst Hellbrück, Stefan Fischer, and Jean-Pierre Hubaux. Traci: An interface for coupling road traffic and network simulators. *11th Communications and Networking Simulation Symposium (CNS)*, 2008.

[28] Hua Wei, Guanjie Zheng, Huaxiu Yao, and Zhenhui Li. Intellilight: A reinforcement learning approach for intelligent traffic light control. In *Proceedings of the 24th ACM SIGKDD International Conference on Knowledge Discovery and Data Mining*, KDD '18, pages 2496–2505, New York, NY, USA, 2018. ACM.

[29] Pengfei Zhu, Xin Li, Pascal Poupart, and Guanghui Miao. On Improving Deep Reinforcement Learning for POMDPs. *arXiv e-prints*, page arXiv:1704.07978, Apr 2017.